A. W. Schreiber, A. I. Signal, and A. W. Thomas
Structure functions in the bag model
Physical Review D, 1991; 44(9):2653-2662

Structure functions in the bag model

A. W. Schreiber
Sektie Kernfysica, Nationaal Instituut voor Kernfysica en Hoge-Energiefysica, P. O. Box 41882, 1009 DB Amsterdam, The Netherlands

A. I. Signal
Department of Physics and Biophysics, Massey University, Palmerston North, New Zealand

A. W. Thomas
Department of Physics and Mathematical Physics, The University of Adelaide, G.P.O. Box 498 Adelaide, South Australia 5001, Australia

(Received 5 June 1991)

In this paper we present calculations of nucleon structure functions in the three-dimensional MIT bag model. The nucleon wave functions are modified by the Peierls Yoccoz projection in order to give eigenstates of the total momentum operator. Pair creation by the probe is taken into account. Without this the quark distributions would not obey normalization requirements. The quark distributions have vanishing support for $x > 1$. The effect of one-gluon exchange, yielding the N-Δ mass splitting, is incorporated. This has significant effects on the d/u ratio as well as the spin-dependent $g_1(x)$ of the neutron. Finally, the results are compared to data after allowing for perturbative QCD evolution.

I. INTRODUCTION

In recent years an extensive examination of the deep structure of nucleons and nuclei has been undertaken. On the experimental side both the old and new European Muon Collaboration (EMC) effects have provided hints that our understanding of this structure was at least incomplete. More recently, high-statistics measurements of the Gottfried sum rule have indicated once again that the simplest pictures of the nucleon are inadequate.

On the theoretical side progress has been much less impressive, with predictions usually only being made after the experimental situation is known. The reason for this is of course that the fundamental theory for the description of the strong interactions (QCD) is poorly understood in the long-distance, nonperturbative region. Nevertheless, at least some of the observed phenomena should not have been unexpected in the light of what is known about the nucleon from low-energy models of the confinement mechanism. Several of these model calculations have been performed. Apart from early attempts in the MIT bag model, especially by Jaffe [1], Hughes [2,3], and Bell [4,5] there have been more recent attempts by Celenza and Shakin [6], Miller and Benesh [7–10], as well as by the Adelaide group. It is the purpose of this article to describe in detail the calculations of the latter. The results for the (1+1)-dimensional version of the model have been presented elsewhere [11–13]. Some results from the three-dimensional version of the model, such as the effects of one-gluon exchange, have been presented previously in a brief format [14–16] but a comprehensive treatment is still missing in the literature.

The paper is organized in the following manner. In Sec. II we begin with a short review of the essential formalism underlying our work, which is completely model independent. In Sec. III, the main part of this paper, we present the calculation within a model where the hadron wave functions consist of products of MIT bag quark wave functions, corrected for center-of-mass motion effects. In Sec. IV we present the straightforward calculations for the case where these wave functions are adjusted for one-gluon-exchange effects. In Sec. V we compare the numerical results with data and in Sec. VI we conclude.

II. REVIEW OF FORMALISM

It is well known that through the use of the operator-product expansion the moments of an arbitrary structure function $\mathcal{F}(x,Q^2)$ may be expressed in terms of a sum of coefficient functions $C_{i,n}(\mu^2,Q^2)$ multiplied by matrix elements $\mathcal{A}_{i,n}(\mu^2)$ [17]:

$$\int_0^1 x^{n-1}\mathcal{F}(x,Q^2)dx = \sum_i \mathcal{A}_{(i,n)}(\mu^2)\mathcal{C}_{(i,n)}(\mu^2,Q^2) \quad . \tag{1}$$

The coefficients $C_{i,n}(\mu^2,Q^2)$ are perturbative corrections which describe the Q^2 evolution of the structure functions and can be reliably calculated by the use of the renormalization-group equations in perturbative QCD.

The matrix elements $\mathcal{A}_{i,n}(\mu^2)$ that yield the dominant contributions at large Q^2 are those of leading twist (2) and have the form, in the $A^+=0$ gauge,

$$\mathcal{A}_{(i,n)} \sim \langle (p,s)_{\mu^2} | \Psi^\dagger(0)\Gamma_i (i\partial^+)^{n-1}\Psi(0) | (p,s)_{\mu^2} \rangle \quad , \tag{2}$$

where the subscripts μ^2 indicate the wave function appropriate at that scale and Γ_i contains Dirac and spin-flavor matrices appropriate to the particular structure function under consideration. (There are in fact additional matrix elements of twist 2 which involve gluonic

operators. We shall not require these.) It is important to note that the matrix elements $\mathcal{A}_{i,n}(\mu^2)$ are independent of Q^2: they depend only on the scale μ^2, which, as opposed to Q^2, need not be large. It is this independence of large momentum transfers that makes their calculation possible in models which would be clearly inadequate for the direct calculation of $\mathcal{F}(x,Q^2)$. (However, μ^2 must be large enough to warrant the use of perturbation theory in the calculation of the coefficient functions.)

The wave functions and operators appearing in Eq. (2) are renormalized ones and so involve the renormalization scale μ_R. Because of our inability to calculate Eq. (2) from QCD we shall make the following ansatz: We shall assume that at the renormalization scale the renormalized wave functions, as well as the renormalized quark field operators, can be approximated by bag wave functions and bag field operators; i.e., we shall calculate the matrix elements (2) within the bag model at the scale $\mu=\mu_R$.

If the matrix elements had been calculated within QCD, μ would be an (arbitrary) parameter in the calculation. The final results for the structure functions would not explicitly depend on it. Within a model calculation, however, it is an undetermined input and can only be obtained by comparison with data. It is common to fix it by using evolution equations to determine at which scale all the hadron's momentum is carried by the quarks, given that only about 50% is carried by them at Q^2 of about 10 GeV^2. This may easily be an untrustworthy procedure as there is no guarantee that the actual momentum distribution, not only its second moment, is fitted by the model. Moreover, in the bag model not all the energy of the hadron is carried by the quarks; in any case, roughly a quarter of it is associated with the bag surface. In short, we shall prefer to fit the scale μ by comparing our prediction for the entire distribution of the valence quarks with the data. All other structure functions are then calculated using this scale as input.

The matrix elements $\mathcal{A}_{i,n}(\mu^2)$ can be written in terms of moments of quark and antiquark distribution functions [18]:

$$q_f^{\uparrow\downarrow}(x)=p^+\sum_n \delta(p^+(1-x)-p_n^+)|\langle n|\Psi_{+,f}(0)|p,s\rangle|^2 \tag{3}$$

and

$$\bar{q}_f^{\uparrow\downarrow}(x)=p^+\sum_n \delta(p^+(1-x)-p_n^+)|\langle n|\Psi_{+,f}^\dagger(0)|p,s\rangle|^2 \ .$$

Here $\uparrow\downarrow$ indicates the helicity projections [$(1\pm\gamma^5)/2$ for the quarks and $(1\mp\gamma^5)/2$ for the antiquarks], the sum is over all intermediate states, f distinguishes flavors, and all $+$ components of momenta k are defined by $k^+=k^0+k^z$. For positive p^+ and p_n^+, $q_f(x)$ and $\bar{q}_f(x)$ are nonzero for $x\leq 1$. They both have support for negative x but as has been shown by Jaffe [19] there are other (semiconnected) contributions in this region, not included in Eq. (3). It is only for $0\leq x\leq 1$ that $q_f(x)$ and $\bar{q}_f(x)$ give the full contribution, and therefore it is only in this region that we have an interpretation of the structure functions in terms of parton distributions.

It is easy to show [18] that Eq. (3) satisfies the normalization condition

$$\int_0^1 dx\,[q_f^{\uparrow\downarrow}(x)-\bar{q}_f^{\uparrow\downarrow}(x)]=N_f^{\uparrow\downarrow}-\bar{N}_f^{\uparrow\downarrow} \ . \tag{4}$$

Here $N_f^{\uparrow\downarrow}$ and $\bar{N}_f^{\uparrow\downarrow}$, roughly speaking, count the numbers of quarks and antiquarks in the target respectively. To prove this, note that because $q(x)$ and $\bar{q}(x)$ do not have support above $x=1$ the upper limit of the integral may be extended to $+\infty$. By writing the δ function appearing in Eq. (3) in its integral representation and translating the field operator Ψ we obtain

$$\int_0^1 dx\,[q_f^{\uparrow\downarrow}(x)-\bar{q}_f^{\uparrow\downarrow}(x)]=\frac{p^+}{2\pi}\int_0^\infty dx\int_{-\infty}^\infty d\xi^-\,e^{-ixp^+\xi^-}[\langle p,s|\Psi_{+,f}^{\uparrow\downarrow\dagger}(\xi^-)\Psi_{+,f}^{\uparrow\downarrow}(0)|p,s\rangle_c - \langle p,s|\Psi_{+,f}^{\uparrow\downarrow}(\xi^-)\Psi_{+,f}^{\uparrow\downarrow\dagger}(0)|p,s\rangle_c] \ . \tag{5}$$

The subscript c indicates a restriction to connected matrix elements. Interchanging the two fermion field operators in the second matrix element introduces a minus sign. Furthermore, by using the translational invariance of this matrix element and changing the integration variables to $-x$ and $-\xi$, we obtain

$$\int_0^1 dx\,\{q_f^{\uparrow\downarrow}(x)-\bar{q}_f^{\uparrow\downarrow}(x)\}=\frac{p^+}{2\pi}\int_{-\infty}^\infty dx\,d\xi^-\,e^{-ixp^+\xi^-}\langle p,s|\Psi_{+,f}^{\uparrow\downarrow\dagger}(\xi^-)\Psi_{+,f}^{\uparrow\downarrow}(0)|p,s\rangle_c = p^+\langle p,s|\Psi_{+,f}^{\uparrow\downarrow\dagger}(0)\Psi_{+,f}^{\uparrow\downarrow}(0)|p,s\rangle_c \tag{6}$$

which counts the number of quarks minus antiquarks, as required. We therefore reiterate: the nonzero support for Eq. (3) for $x\leq 0$ in model calculations should not be seen as a problem that needs to somehow be overcome; contributions at negative x are simply irrelevant. However, what may be a problem in model calculations, including the one presented here, is that some of the properties that are assumed of the matrix elements that lead to expression (6) may not be satisfied. In particular the matrix elements should be translationally invariant, the set of intermediate states should be a complete set, the interchange of field operators that is required in arriving at Eq. (6) should be valid, and both the intermediate and initial states should be eigenstates of the operator p^+. In the model calculation that we present here the last requirement is not satisfied exactly and we therefore do not

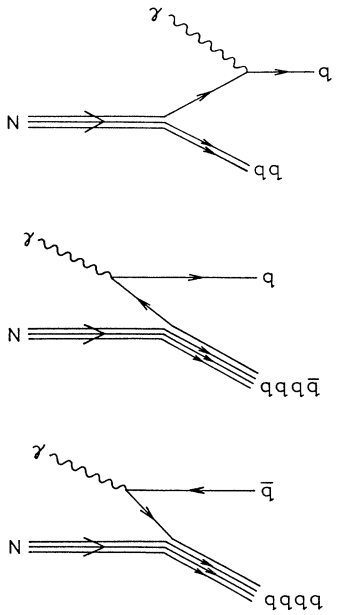

FIG. 1. Processes contributing to the twist-2 piece of $\mathcal{A}$.

automatically obtain the correct normalization. We shall return to this point later.

Let us now look in more detail at the quark and antiquark distributions in Eq. (3). The field operators Ψ and $\Psi^\dagger$, when expanded in a complete set of states, each gives two distinct contributions. Ψ may destroy a quark contained in the initial state leaving a two-quark intermediate state, or it may create an antiquark resulting in a three-quark–one-antiquark intermediate state. Similarly $\Psi^\dagger$ may take an antiquark out of the initial state (this, however, will give no contribution for our choice of model wave function, which shall consist of only three valence quarks) or insert a quark. These processes are depicted in Fig. 1. We know of no reason why the processes with the four-quark (or one-antiquark, three-quark) intermediate states should not contribute to the scattering process. Certainly within the model that we describe in the next section they formally give a contribution, although not a large one.

III. DISTRIBUTIONS IN THE BARE BAG

A. The two-quark component

Let us concentrate first on those contributions with a two-quark intermediate state. We define the action of the operator Ψ on a three-quark state through

$$\Psi(\mathbf{x})|\mathbf{x}_1\mathbf{x}_2\mathbf{x}_3\rangle=\delta(\mathbf{x}-\mathbf{x}_3)|\mathbf{x}_1\mathbf{x}_2\rangle+\text{permutations} \tag{7}$$

and similarly for two-quark states. Inserting complete sets of states in Eq. (3) we obtain straightforwardly

$$q_f^{\uparrow\downarrow}(x)=\frac{M}{(2\pi)^3}\sum_{n,\alpha}\langle\mu|P_{f,\alpha}|\mu\rangle\delta(M(1-x)-p_n^+)\left|\int d\mathbf{x}_1\,d\mathbf{x}_2\langle\mathbf{p}_n|\mathbf{x}_1\mathbf{x}_2\rangle\langle\mathbf{x}_1\mathbf{x}_2 0_\alpha^{\uparrow\downarrow}|0\rangle\right|^2 . \tag{8}$$

Here $|\mu\rangle$ is the spin-flavor wave function of the initial state which we have taken to be at rest and $P_{f,\alpha}$ is a projection operator onto flavor f and any other required quantum numbers α. In our case, where we assume that all initial quarks are in the lowest-energy states, α may be taken to be synonymous with the quark spin projection m. Unless the initial wave function consists of three quarks moving only in the z direction (i.e., the naive parton model), there will be a contribution from $m=+\frac{1}{2}$ and $m=-\frac{1}{2}$ for both $q_f^{\uparrow}(x)$ and $q_f^{\downarrow}(x)$ separately.

Let us now describe our choice for the model wave function. We choose wave functions inspired by those of the MIT bag; however, we modify these by a projection, the Peierls-Yoccoz projection [20], which ensures that the wave functions are momentum eigenstates and hence the translational invariance of the matrix elements appearing in Eqs. (5) and (6). Explicitly we have in the coordinate representation

$$\langle\mathbf{x}_1\mathbf{x}_2\mathbf{x}_3|\mathbf{p}\rangle=\frac{1}{\phi_3(\mathbf{p})}\int d\mathbf{R}\,e^{i\mathbf{p}\cdot\mathbf{R}}\Psi(\mathbf{x}_1-\mathbf{R})\Psi(\mathbf{x}_2-\mathbf{R})\times\Psi(\mathbf{x}_3-\mathbf{R}) . \tag{9}$$

Here $\phi_3(\mathbf{p})$ is given by the normalization requirement

$$\langle\mathbf{p}|\mathbf{p}'\rangle=(2\pi)^3\delta(\mathbf{p}-\mathbf{p}') \tag{10}$$

or, explicitly,

$$|\phi_3(\mathbf{p})|^2=\int d\mathbf{x}\,e^{-i\mathbf{p}\cdot\mathbf{x}}\left[\int dy\,\Psi^\dagger(y-x)\Psi(y)\right]^3 . \tag{11}$$

The wave function for the diquark state has an analogous normalization.

Before we make use of this wave function let us remind the reader of the deficiencies of the Peierls-Yoccoz procedure. Although it creates a momentum eigenstate, there still is an unphysical dependence on the momentum in the internal wave function. It is possible to eliminate this through a further projection, the Peierls-Thouless projection [21]; however, the wave functions that result are in practice completely intractable to work with. Furthermore, the Peierls-Yoccoz projection is a nonrelativistic approximation and is not equivalent to a boost. For the initial state, which is at rest, this is probably a reasonable assumption. For the intermediate state, the approximation is only valid for the region where $|p_n|<M_n$ (M_n is the mass of the intermediate two-particle state). As we shall see shortly, this corresponds to the region of x less than about 0.6–0.7.

Using Eq. (9) in Eq. (8) gives

$$q_f^{\uparrow\downarrow}(x)=\frac{M}{(2\pi)^3}\sum_m \langle\mu|P_{f,m}|\mu\rangle \int d\mathbf{p}_n \frac{|\phi_2(\mathbf{p}_n)|^2}{|\phi_3(\mathbf{0})|^2}\delta(M(1-x)-p_n^+)|\tilde{\Psi}_{+,f}^{\uparrow\downarrow}(\mathbf{p}_n)|^2 . \tag{12}$$

Here

$$\tilde{\Psi}_{+,f}^{\uparrow\downarrow}(\mathbf{p}_n)\equiv\int d\mathbf{x}\, e^{i\mathbf{p}_n\cdot\mathbf{x}}\Psi_{+,f}^{\uparrow\downarrow}(\mathbf{x}) . \tag{13}$$

It is easiest to do the integration by choosing the magnitude of $\mathbf{p}_n$ and its transverse components $\mathbf{p}_n^\perp$ as integration variables, as well as using the δ function to do the $\mathbf{p}_n^\perp$ integration. One obtains

$$\int d\mathbf{p}_n\,\delta(M(1-x)-p_n^+) = 2\pi\int_{|[M^2(1-x)^2-M_n^2]/2M(1-x)|}^{\infty} p_n\,dp_n , \tag{14}$$

where

$$\mathbf{p}_\perp^2=2M(1-x)\sqrt{M_n^2+\mathbf{p}_n^2}-M^2(1-x)^2-M_n^2 \tag{15}$$

is understood. Equation (12) therefore becomes

$$q_f^{\uparrow\downarrow}(x)=\frac{M}{(2\pi)^2}\sum_m\langle\mu|P_{f,m}|\mu\rangle\int_{|[M^2(1-x)^2-M_n^2]/2M(1-x)|}^{\infty} p_n dp_n \frac{|\phi_2(\mathbf{p}_n)|^2}{|\phi_3(\mathbf{p})|^2}|\Psi_m^{\uparrow\downarrow}(\mathbf{p}_n)|^2 . \tag{16}$$

It is from this equation that one can read off when one might expect the nonrelativistic approximation for the intermediate state to be a reasonable one. The main contribution to the integral comes from the region of small p_n so the nonrelativistic approximation should be valid as long as the lower limit of the p_n integration is less than M_n—this is true for x less than about 0.7 for $M_n\approx\frac{3}{4}M$.

The evaluation of the normalizations $\phi_2(\mathbf{p}_n)$ and $\phi_3(\mathbf{0})$, as well as $\tilde{\Psi}_m^{\uparrow\downarrow}(\mathbf{p}_n)$, is straightforward but tedious. Using the MIT bag wave functions with lowest energy,

$$\Psi_m(x)=N\begin{pmatrix} j_0\left[\frac{\Omega|x|}{R}\right]\chi_m \\ i\boldsymbol{\sigma}\cdot\hat{\mathbf{x}}j_1\left[\frac{\Omega|x|}{R}\right]\chi_m\end{pmatrix}\Theta(R-|x|) , \tag{17}$$

where R is the bag radius,

$$N^2=\frac{1}{4\pi R^3}\frac{\Omega^4}{\Omega^2-\sin^2\Omega} \tag{18}$$

and Ω is the lowest-energy solution of

$$j_0(\Omega)=j_1(\Omega) , \quad \text{i.e.,} \quad \Omega\approx 2.04 , \tag{19}$$

one obtains

$$|\phi_2(\mathbf{p}_n)|^2=\frac{4\pi R^3}{U(\Omega^2-\sin^2\Omega)^2}\int_0^\Omega\frac{dv}{v}\sin\frac{2uv}{\Omega}T^2(v) \tag{20}$$

and

$$|\phi_3(\mathbf{0})|^2=\frac{4\pi R^3}{(\Omega^2-\sin^2\Omega)^3}\int_0^\Omega\frac{dv}{v}T^3(v) , \tag{21}$$

where

$$T(v)=\left[\Omega-\frac{\sin^2\Omega}{\Omega}-v\right]\sin 2v-\left[\frac{1}{2}+\frac{\sin 2\Omega}{2\Omega}\right]\cos 2v + \frac{1}{2}+\frac{\sin 2\Omega}{2\Omega}-\frac{\sin^2\Omega}{\Omega^2}v^2 \tag{22}$$

and we have made the substitutions

$$v=\frac{|\mathbf{x}|\Omega}{2R} , \quad u=|\mathbf{p}_n|R . \tag{23}$$

The Fourier transform of Ψ becomes

$$|\Psi_m^{\uparrow\downarrow}(\mathbf{p}_n)|^2=\tfrac{1}{2}[f(\mathbf{p}_n)\pm(-1)^{m+3/2}g(\mathbf{p}_n)] , \tag{24}$$

where

$$f(\mathbf{p}_n)=\frac{\pi R^3}{2}\frac{1}{(\Omega^2-\sin^2\Omega)}\times\left[s_1^2(u)+2\frac{p_n^z}{|\mathbf{p}_n|}s_1(u)s_2(u)+s_2^2(u)\right] \tag{25}$$

and

$$g(\mathbf{p}_n)=\frac{\pi R^3}{2}\frac{1}{\Omega^2-\sin^2\Omega}\left\{s_1^2(u)+2\frac{p_n^z}{|\mathbf{p}_n|}s_1(u)s_2(u)+\left[1-2\left[\frac{p_n^\perp}{|\mathbf{p}_n|}\right]^2\right]s_2^2(u)\right\} . \tag{26}$$

Here

$$s_1(u)=\frac{1}{u}\left[\frac{\sin(u-\Omega)}{u-\Omega}-\frac{\sin(u+\Omega)}{u+\Omega}\right] \tag{27}$$

and

$$s_2(u)=2j_0(\Omega)j_1(u)-\frac{u}{\Omega}s_1(u) . \tag{28}$$

If we assume that $|\mu\rangle$ is the 56-plet SU(6) wave function for the proton with $m=+\frac{1}{2}$ we get, using the matrix elements

$$\begin{aligned}
&\langle\mu|P_{u,+\frac{1}{2}}|\mu\rangle=\tfrac{5}{3} ,\\
&\langle\mu|P_{u,-\frac{1}{2}}|\mu\rangle=\tfrac{1}{3} ,\\
&\langle\mu|P_{d,+\frac{1}{2}}|\mu\rangle=\tfrac{1}{3} ,\\
&\langle\mu|P_{d,-\frac{1}{2}}|\mu\rangle=\tfrac{2}{3} ,
\end{aligned} \tag{29}$$

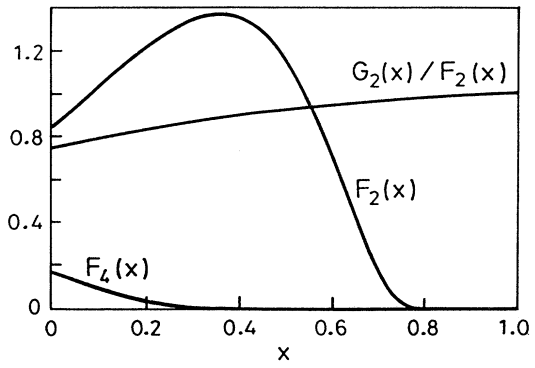

FIG. 2. Quark distributions in the bare bag.

that

$$u^{\uparrow\downarrow}_{(2)}(x)=F_{(2)}(x)\pm\tfrac{2}{3}G_{(2)}(x) \tag{30}$$

and

$$d^{\uparrow\downarrow}_{(2)}(x)=\tfrac{1}{2}F_{(2)}(x)\mp\tfrac{1}{6}G_{(2)}(x)\ , \tag{31}$$

where $F_{(2)}(x)$ and $G_{(2)}(x)$ correspond to those parts of Eq. (12) originating in Eqs. (25) and (26), respectively. [u and d refer to the up- and down-quark distributions. The subscript (2) reminds us that we have up to now only calculated the contributions of the two-quark intermediate state.]

We note that the formalism predicts quite naturally a different x behavior of the helicity-dependent from that of the helicity-independent structure functions. This difference is due to the nonzero $\mathbf{p}_\perp$ of the quarks and is therefore absent in the naive parton model. Numerically, for a bag radius of 0.8 F and an intermediate diquark mass of $M_n=\frac{3}{4}M$, $F_{(2)}(x)$ and $G_{(2)}(x)/F_{(2)}(x)$ are shown in Fig. 2. $F_{(2)}(x)$ and $G_{(2)}(x)$ are peaked near $x=1-M_n/M$ and we see that the difference between the helicity-dependent and helicity-independent distributions is greatest in the small-x region, i.e., where $|\mathbf{p}_\perp|$ is large compared with p^+.

B. Normalization of the two-quark component and $|g_A/g_V|$

As expected, the distributions $F_{(2)}(x)$ and $G_{(2)}(x)$ do not saturate the normalization requirement [Eq. (4)]. Before we discuss the contributions from the four-particle intermediate states we want to draw attention to an interesting property of $F_{(2)}(x)$ and $G_{(2)}(x)$. Their integrals from $-\infty$ to ∞ (or, equivalently, from $-\infty$ to 1) can be evaluated analytically and are given by

$$\int_{-\infty}^{1}F_{(2)}(x)dx=1 \tag{32}$$

and

$$\int_{-\infty}^{1}G_{(2)}(x)dx=\frac{\int[I_T(\mathbf{x})+I_B(\mathbf{x})]^2[I_T(\mathbf{x})-\frac{1}{3}I_B(\mathbf{x})]d\mathbf{x}}{\int[I_T(\mathbf{x})+I_B(\mathbf{x})]^3d\mathbf{x}}$$
$$\simeq 0.789 \quad \text{for } \Omega=2.04\ . \tag{33}$$

Here $I_T(\mathbf{x})$ and $I_B(\mathbf{x})$ are

$$I_{T,B}(\mathbf{x})=\int d\mathbf{y}\,\Psi^\dagger_{T,B}(\mathbf{y}-\mathbf{x})\Psi_{T,B}(\mathbf{y})\ . \tag{34}$$

$\Psi_{T,B}$ refers to the top and bottom parts of the spinors (17), respectively. The important point about Eqs. (32) and (33) is that they are independent of all parameters except, in the case of the latter, the quark energy Ω.

Let us consider what would happen if we allowed the bag radius R to become very large. In this case the spread of quark momenta around $\mathbf{p}_q=\mathbf{0}$ decreases and the distributions $F_{(2)}(x)$ and $G_{(2)}(x)$ tend towards δ functions at $x=1-M_N/M$. This also is true for the four-particle intermediate states, except that in this case, because $M_N>M$, the δ functions move to negative x and hence do not contribute to the normalization. We therefore conclude that the integrals (32) and (33) over all x at finite R yield the same results as the integrals from 0 to 1 of all contributions of Fig. 1; i.e., the renormalization requirement of Eq. (4) is satisfied by Eqs. (32) and (33). They therefore give a useful guide as to how much of the normalization is carried by the contributions from the four-quark intermediate states.

The reduction of the integral of $G_{(2)}(x)$ from 1 is indicative of the spin dilution in relativistic models of nucleon structure. In fact, with the use of the Bjorken sum rule we may write down the value of the axial-vector coupling constant g_A, i.e.,

$$\left|\frac{g_A}{g_V}\right|=\int_0^1(\Delta u-\Delta d)dx$$
$$=\tfrac{5}{3}\int_{-\infty}^{1}G_{(2)}(x)dx=1.32 \tag{35}$$

This is larger than the famous $\frac{5}{3}\Omega/3(\Omega-1)=1.09$ of the MIT bag model because we have included center-of-mass motion corrections through the use of the Peierls-Yoccoz projection.

C. The four-quark intermediate states

We now turn to the other processes depicted in Fig. 1. Their contributions can be calculated in the same manner as those of the two-quark intermediate states and are given by

$$q^{\uparrow\downarrow}_{(4),f}(x)=\frac{M}{(2\pi)^3}\sum_m\langle\mu|P^{(\bar q)}_{f,m}|\mu\rangle\int d\mathbf{p}_n\frac{|\phi_4(\mathbf{p}_n)|^2}{|\phi_3(\mathbf{0})|^2}\delta(M(1-x)-p_n^+)|\tilde\Psi^{\uparrow\downarrow}_{(\bar q)+,m}(\mathbf{p}_n)|^2 \tag{36}$$

for the 3-quark–1-antiquark intermediate state, and

$$\bar{q}^{\uparrow\downarrow}_{(4),f}(x)=\frac{M}{(2\pi)^3}\langle\mu|P^{(q)}_{f,m}|\mu\rangle\int d\mathbf{p}_n\frac{|\phi_4(\mathbf{p}_n)|^2}{|\phi_3(\mathbf{0})|^2}\delta(M(1-x)-p_n^+)|\tilde{\Psi}^{\uparrow\downarrow\dagger}_{(q)+,m}(\mathbf{p}_n)|^2 \tag{37}$$

for the 4-quark intermediate state. The spinor $\tilde{\Psi}^{\uparrow\downarrow}_{(\bar{q}),m}(\mathbf{p}_n)$ is that corresponding to an antiquark bag wave function

$$\Psi^{\uparrow\downarrow}_{(\bar{q}),m}(\mathbf{x})=N\begin{bmatrix}-i\boldsymbol{\sigma}\cdot\hat{\mathbf{r}}j_1\left[\frac{\Omega r}{R}\right]\chi_m\\ j_0\left[\frac{\Omega R}{R}\right]\chi_m\end{bmatrix}\Theta(R-r) \tag{38}$$

and yields

$$|\tilde{\Psi}^{\uparrow\downarrow}_{(\bar{q})+,m}(\mathbf{p}_n)|^2=\tfrac{1}{2}[f(-\mathbf{p}_n)\mp(-1)^{m+3/2}g(-\mathbf{p}_n)]\ , \tag{39}$$

where f and g have been defined previously.

The integral in Eq. (37) involves the Hermitian conjugate of the quark wave function and gives the same contribution as that in Eq. (36) because

$$|\tilde{\Psi}^{\uparrow\downarrow\dagger}_{(q)+,m}(\mathbf{p}_n)|^2=|\tilde{\Psi}^{\uparrow\downarrow}_{(\bar{q})+,m}(-\mathbf{p}_n)|^2\ . \tag{40}$$

The projection operators appearing in Eqs. (36) and (37) count the number of possible quark or antiquark insertions allowed by the Pauli principle:

$$\begin{aligned}\langle\mu|P^{(\bar{q})}_{u,+1/2}|\mu\rangle&=\langle\mu|P^{(\bar{q})}_{u,-1/2}|\mu\rangle=\langle\mu|P^{(\bar{q})}_{d,+1/2}|\mu\rangle\\&=\langle\mu|P^{(\bar{q})}_{d,-1/2}|\mu\rangle=3\end{aligned} \tag{41}$$

and

$$\begin{aligned}\langle\mu|P^{(q)}_{u,+1/2}|\mu\rangle&=\tfrac{4}{3}\ ,\\ \langle\mu|P^{(q)}_{u,-1/2}|\mu\rangle&=\tfrac{8}{3}\ ,\\ \langle\mu|P^{(q)}_{d,+1/2}|\mu\rangle&=\tfrac{8}{3}\ ,\\ \langle\mu|P^{(q)}_{d,-1/2}|\mu\rangle&=\tfrac{7}{3}\ .\end{aligned} \tag{42}$$

Here we have again assumed SU(6) proton wave functions. As expected, the number of up quarks that can be inserted at four (two states being already occupied), while the number of down quarks is five.

Finally then, the contributions from the four-quark intermediate states can be written down in an analogous form to Eqs. (30) and (31): i.e.,

$$u^{\uparrow\downarrow}_{(4)}(x)=d^{\uparrow\downarrow}_{(4)}(x)=3F_{(4)}(x)$$

and

$$\begin{aligned}\bar{u}^{\uparrow\downarrow}_{(4)}(x)&=2F_{(4)}(x)\pm\tfrac{2}{3}G_{(4)}(x)\ ,\\ \bar{d}^{\uparrow\downarrow}_{(4)}(x)&=\tfrac{5}{2}F_{(4)}(x)\mp\tfrac{1}{6}G_{(4)}(x)\ .\end{aligned} \tag{43}$$

$F_{(4)}$ and $G_{(4)}$ need not be written down explicitly; they have the same form as $F_{(2)}$ and $G_{(2)}$, with the replacements of ϕ_2 by ϕ_4 and $\tilde{\Psi}^{\uparrow\downarrow}_{+,m}(\mathbf{p}_n)$ by $\tilde{\Psi}^{\uparrow\downarrow}_{+,m}(-\mathbf{p}_n)$, as indicated in the above discussion. For a four-particle state mass of $M_N=\frac{5}{4}M$, and again a bag radius of 0.8 fm, $F_{(4)}$ is shown in Fig. 2. It is very much smaller than $F_{(2)}$ and concentrated at small x, with a falloff reminiscent of a sea distribution.

D. Normalization revisited

We are now in a position to evaluate the normalization [Eq. (4)] explicitly. Using Eqs. (30), (31), and (43) we get

$$\begin{aligned}\tfrac{1}{2}\int_0^1 dx\,[u_{(2)}(x)+u_{(4)}(x)-\bar{u}_{(4)}(x)]&\\ =\int_0^1 dx\,[d_{(2)}(x)+d_{(4)}(x)-\bar{d}_{(4)}(x)]&\\ =\int_0^1 dx\,[F_{(2)}(x)+F_{(4)}(x)]\ .&\end{aligned} \tag{44}$$

The numerical values for various bag radii are tabulated in Table I. The intermediate state masses have been kept fixed at $\frac{3}{4}$ and $\frac{5}{4}$ of the proton mass for the di- and four-quark masses respectively. We see that for reasonable nucleon radii of $\sim$0.8 fm the normalization consists of about 75% from the two-quark intermediate state and 2% from the four-quark (-antiquark) states. About 23% is missing.

Both the integral of $F_{(2)}(x)$ as well as that of $F_{(4)}(x)$ are a function of the mass of the relevant intermediate state. Without a way to calculate the intermediate-state masses in a consistent manner within the model it is impossible to satisfy the normalization requirement explicitly. The best we can do is to adjust the masses in order to saturate the integral. Alternatively, and this is the course that will be taken when we compare results with data, we shall just parametrize the four-particle contribution such that the normalization is satisfied [$(1-x)^7$ gives an excellent approximation to the shape shown in Fig. 2].

It is clear that the arbitrariness of this procedure will introduce some uncertainty into the final results. Because of the shape of the four-quark contribution this uncertainty is concentrated at small x. In fact, after the

TABLE I. The normalizations of $F_{(2)}$ and $F_{(4)}$, using $M_n=\frac{3}{4}$ and $\frac{5}{4}$ for the two- and four-particle intermediate states, respectively.

R (fm)	$\int_0^1 dx\,F_{(2)}(x)$	$\int_0^1 dx\,F_{(4)}(x)$	$\int_0^1 dx\,[F_{(2)}(x)+F_{(4)}(x)]$
0.2	0.32	0.026	0.35
0.6	0.65	0.029	0.68
0.8	0.75	0.023	0.77
1.0	0.82	0.018	0.84
2.0	0.98	0.003	0.98

model distributions have been evolved to a scale where they can be compared with data, say $Q^2=10$ GeV^2, the affected region moves to yet smaller x. We must therefore conclude that the results obtained at small x will be less reliable than those at larger x and hence care should be taken not to read too much into the results in this region.

IV. M_N AND ONE-GLUON EXCHANGE

Having presented the basic formalism in the previous section, we now turn to refinements of the model. One physical effect that we have neglected up to now, but that has been known for a long time to affect the spin-flavor dependence of the quark distributions [22], is one-gluon exchange. Specifically, it is clear from Eqs. (30) and (31) that so far all spin-independent distributions have the same shape [i.e., that of $F_{(2)}(x)$], and similarly the spin-dependent distributions all have a shape proportional to $G_{(2)}(x)$ [we neglect here the modifications at small x due to $F_{(4)}(x)$ and $G_{(4)}(x)$, respectively]. We would therefore predict that quantities such as $d_v(x)/u_v(x)$ are constant (the subscript v here stands for valence), while the asymmetry $2xg_1(x)/F_2(x)$ will have the same shape as $G_{(2)}(x)/F_{(2)}(x)$, shown in Fig. 2. Both of these predictions are in stark contrast to the experimental situation.

Because of its importance, the effect of the one-gluon-exchange mechanism is frequently built into model descriptions. It manifests itself in a similar way as the hyperfine splitting in atomic physics, in that the spectator diquark mass depends on whether it is in its spin-singlet (lower-mass) or spin-triplet (higher-mass) configuration. The magnitude of the splitting can be obtained, for example, from the $N-\Delta$ mass difference (assuming that this has the same origin). Explicitly, one finds that the spin-triplet state is around 50 MeV heavier than a diquark without hyperfine splitting, and the singlet state is 150 MeV lighter. The unsplit diquark mass we again assume to be roughly the viral theorem is $\frac{3}{4}$ of the (unsplit) baryon's mass. Further details may be found in [14] (an identical procedure is also followed in a recent paper by Meyer and Mulers [23]).

The spin-flavor matrix elements appearing in Eq. (16) depend on the spin state of the spectator quarks and are given by

$$\begin{aligned}
&\langle \mu,s=0|P_{u,+1/2}|\mu,s=0\rangle=\tfrac{3}{2}\ , \quad \langle \mu,s=1|P_{u,+1/2}|\mu,s=1\rangle=\tfrac{1}{6}\ ,\\
&\langle \mu,s=0|P_{u,-1/2}|\mu,s=0\rangle=0\ , \quad \langle \mu,s=1|P_{u,-1/2}|\mu,s=1\rangle=\tfrac{1}{3}\ ,\\
&\langle \mu,s=0|P_{d,+1/2}|\mu,s=0\rangle=0\ , \quad \langle \mu,s=1|P_{d,+1/2}|\mu,s=1\rangle=\tfrac{1}{3}\ ,\\
&\langle \mu,s=0|P_{d,-1/2}|\mu,s=0\rangle=0\ , \quad \langle \mu,s=1|P_{d,-1/2}|\mu,s=1\rangle=\tfrac{2}{3}\ .
\end{aligned} \tag{45}$$

This gives the quark distributions

$$\begin{aligned}
u^{\uparrow\downarrow}_{(2)}(x)&=[\tfrac{3}{4}F_s(x)+\tfrac{1}{4}F_v(x)]\pm\tfrac{2}{3}[\tfrac{9}{8}G_s(x)-\tfrac{1}{8}G_v(x)]\ ,\\
d^{\uparrow\downarrow}_{(2)}(x)&=\tfrac{1}{2}F_v(x)\mp\tfrac{1}{6}G_v(x)\ ,
\end{aligned} \tag{46}$$

where the subscripts s and v refer to the relevant intermediate state masses to be used when evaluating $F_{(2)}(x)$ and $G_{(2)}(x)$.

We note that the distribution of u quarks is dominated by the scalar (i.e., lower mass) intermediate state while the d quark is entirely given by the vector (i.e., higher mass) intermediate state. As we saw in the previous section the distributions peak near $x=1-M_N/M$, so it follows that the u-quark distribution peaks at a larger x than that of the d quark, leading to a vanishing $d_v(x)/u_v(x)$ ratio as $x\to 1$. Similarly, the asymmetry can be written explicitly as

$$\frac{2xg_1(x)}{F_2(x)}=\frac{6G_s(x)-G_v(x)}{6F_s(x)+3F_v(x)}\to 1 \quad \text{as } x\to 1\ . \tag{47}$$

In Fig. 3 we show some typical results for these two quantities, using a bag radius of 0.8 fm and diquark masses of 650 and 850 MeV for the singlet and vector diquark case, respectively.

V. COMPARISON OF MODEL CALCULATIONS WITH DATA

Given the model for the matrix element $\mathcal{A}_{(n)}$ that has been described in the previous sections, we may now proceed to compare some of the predictions with data. As pointed out earlier, this requires a knowledge of the momentum scale μ at which the bag mode is expected to

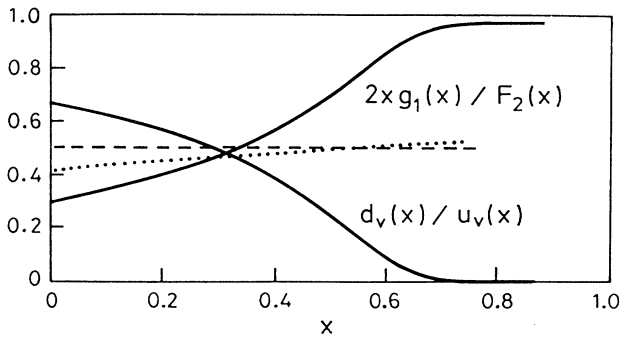

FIG. 3. Asymmetry and d/u ratio with inclusion of hyperfine splitting. The dashed (dotted) line is the d/u ratio (asymmetry) without the one-gluon exchange.

be a reasonable approximation to QCD. We fit this scale by comparing the predictions for the (isospin-singlet) valence distribution to data. Having fixed the scale we are then free to evaluate all other quantities that may be of interest.

Before we do this we need to decide what to do about the normalization of the distributions. Our procedure will be as follows: We shall choose parameters (bag radius, diquark-state mass) for the two-quark component and shall then add in a term, corresponding to the four-quark component, to fix the normalizations. For simplicity we shall mimic the behavior of the four-quark term by $(1-x)^7$. This is a very good approximation to the actual behavior of the four-quark term shown in Fig. 2. The qualitative behavior of the results is not affected greatly by the precise form of this function, especially for $x > 0.3$. We shall compare our results with a recent compilation by Charchula *et al.* [24] of four different parametrizations of data (all rescaled to $Q^2=10$ GeV^2): (1) Eichten-Hinchliffe-Lane-Quigg, set I [25] (solid curves); (2) Martin-Roberts-Stirling, set I [26] (dotted curves); (3) Duke-Ownes, set I [27] (dashed curves); (4) Diemoz-Ferroni-Longo, set II [28] (dot-dashed curves). The difference between these parametrizations we take to be indicative of the experimental uncertainties.

One obtains reasonable fits to the valence distribution for bag radii of around 0.6 to 0.8 fm and scalar (vector) diquark masses of 650 (850) to 850 (1050) MeV. In Fig. 4 we show a typical result, corresponding to $R=0.6$ fm, $M_s=550$ MeV, $M_v=750$ MeV. For these parameters μ is rather low, about 0.26 GeV. Higher values of μ, up to 0.46 GeV, are necessary if the diquark masses are towards the upper part of the above range. Using $\Lambda_{\rm QCD}=200$ MeV, this corresponds to a coupling constant α at the scale μ of 2.5 and 0.8, respectively. Both values are rather higher than one would comfortably like them to be for leading-order QCD corrections to be dominant. Similar [7,23] values of $\alpha(\mu)$, or even higher [29] ones, have been found in other model calculations.

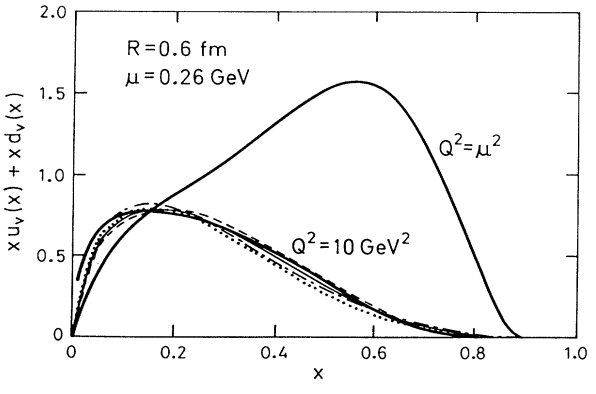

FIG. 4. The valence distribution for the bare bag, corrected for one-gluon exchange. The thick curves correspond to the theoretical results, both at the model scale μ and at $Q^2=10$ GeV^2. The light curves are parametrizations of data (see text).

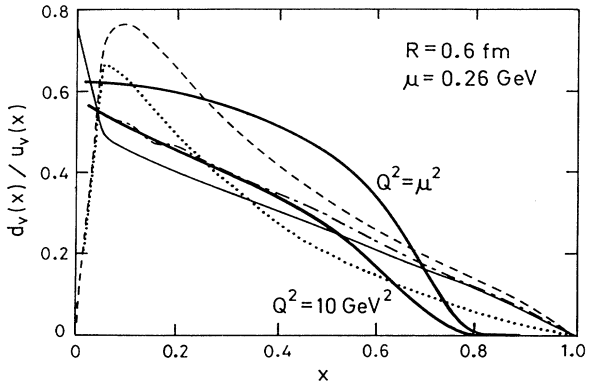

FIG. 5. The ratio of valence distributions of the down and up quarks for the same parameters as those in Fig. 4.

Using this value of μ we may now predict other structure functions without introducing any more parameters. In Fig. 5 we show the ratio $u_v(x,Q^2)/d_v(x,Q^2)$ plotted against the parametrizations of the data. There is quite reasonable agreement for most of the range of x, except in the large-x region. It is in this region where the sharpness of the bag boundary makes itself felt, something that was especially noticeable in the two-dimensional calculation of Signal *et al.* [30].

In Fig. 6 the corresponding results for $g_1^p(x)$ are shown, together with the available data from the European Muon Collaboration (EMC) [31,32]. For $x > 0.2$ there is good agreement; however, for small x the prediction is significantly above the data. At present it is not possible to state with certainty what the origin of this discrepancy is, but let us make several remarks. In the model presented here the spin of the proton is carried completely by the quarks [the integral of $g_1^p(x)$ is $\frac{5}{18}\int dx\, G_{(2)} \approx 0.22$] and it is well known that the data are probably in disagreement with this. Efremov, Teryaev, Altarelli, Ross, and others [33–36] have shown that there is an anomalous gluon contribution to the integral of $g_1^p(x)$

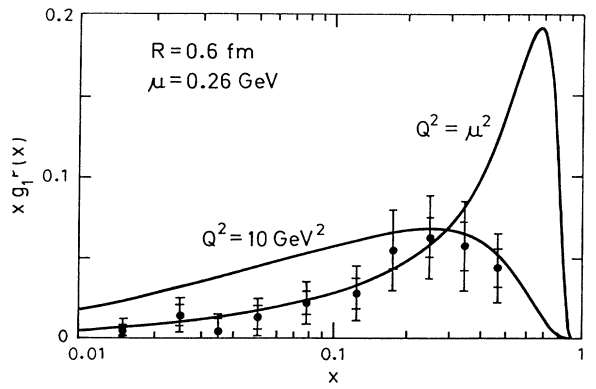

FIG. 6. $g_1^p(x)$ for the same parameters as those in Fig. 4. The data are that of the EMC.

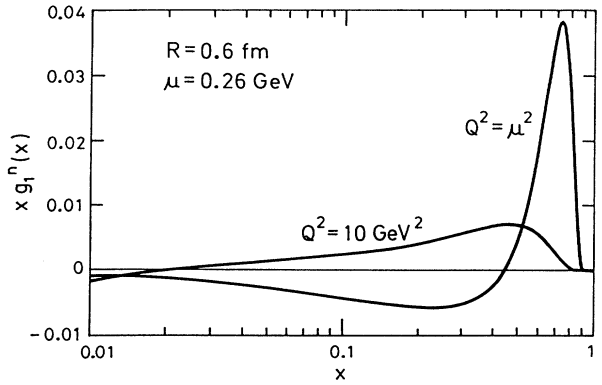

FIG. 7. $g_1^n(x)$ for the same parameters as those in Fig. 4.

due to the Adler-Bell-Jackiw anomaly [37,38] and it has been suggested that via this mechanism the dynamically generated glue of leading (and next-to-leading) order QCD evolution is sufficient [39,40] to explain the discrepancy. Even if one accepts the validity of this mechanism (for contrary points of view see [41–43]), with no polarized gluon at the bag scale and the above value of μ, the gluonic contribution to the integral would be about -0.04, which is not sufficient to bring the theoretical value into agreement with the experimental one of 0.126 ± 0.010 (stat) ±0.015 (syst). A value of μ sufficiently close to $\Lambda_{\rm QCD}$ would enable sufficient gluons to be generated; however, it would also shift all calculated structure functions to smaller x. An inspection of Fig. 4, for example, indicates that this will probably cause serious disagreement with experiment for $F_3(x)$. Further discussion of this point may be found in [44].

A decrease in $g_1^p(x)$ for small x could be achieved by raising μ. This would be the effect of the correction to the nucleon wave function from the inclusion of a pion cloud. The pions carry some of the momentum of the nucleon at the scale μ and so the range of evolution would have to be decreased compared with the case considered here, i.e., where the valence quarks (and the bag surface) carry all of the momentum of the proton at the model scale. The precise correction to $g_1(x)$ will depend on the change to the spin-isospin structure of the wave function. This calculation is presently being done and will be published elsewhere.

Finally, in Fig. 7 we show the results for $g_1^n(x)$. In an SU(6)-symmetric model $g_1^n(x)$ is zero everywhere. The splitting arising from one-gluon exchange causes it to become finite, although the first moment still vanishes. [The QCD evolution also induces a small value of $g_1^n(x,Q^2)$, even if $g_1^n(x,\mu^2)=0$, because the singlet and nonsinglet parts evolve differently. The effect is typically $\frac{1}{3}$ of the size of the effect considered here.] The large peak in $g_1^n(x,\mu^2)$ at large x as well as the value of μ causes the region where $g_1^n(x,Q^2=10\ \text{GeV}^2)$ is negative to move to rather small x. It will be interesting to compare this with data. A significantly larger value for the intercept would indicate that the bag-model scale should not be as low as we have made it here, once again an indication that pionic corrections to the nucleon wave function are important. Apart from changing the scale μ these cause further change to the SU(6) wave function of the nucleon. The changes to $g_1^n(x)$ are of the same order as the ones considered here (indeed they even result in a nonzero value for the integral).

VI. CONCLUSION

In this paper we have presented a calculation of nucleon structure functions from bag model wave functions. The wave functions we have used are translationally invariant and the structure functions we have calculated have nonzero support only between $0\le x\le 1$. An important effect is the inclusion of four-particle intermediate states, without which the quark distributions would not obey normalization requirements. The effect of the hyperfine splitting due to one-gluon exchange has also been incorporated. This produces significant effects, especially in ratios of structure functions or quark distributions.

The results have been compared with parametrizations of data. It is encouraging that despite the crudity of the model there is qualitative agreement between theory and experiment. There are, however, some potentially serious discrepancies, essentially at low x. To understand these, two improvements are essential. At present, the relative importance of the contributions from the 2- and 4-quark intermediate state can only be estimated because of poor knowledge of their masses. Furthermore, a pion cloud will carry some of the momentum of the nucleon, as well as change its spin-isospin distribution. It is essential to include this in order to make further progress—especially if one intends to make meaningful predictions for $g_1^n(x)$.

ACKNOWLEDGMENTS

One of us (A.W.S.) acknowledges many useful conversations with members of the NIKHEF theory group about these calculations and financial support from the University of Adelaide. This work was supported by the Australian Research Council.

[1] R. L. Jaffe, Phys Rev D **11**, 1953 (1975).
[2] R. J. Hughes, Phys. Rev. D **16**, 622 (1977).
[3] J. A. Bartelski, Phys. Rev. D **20**, 1229 (1979).
[4] J. S. Bell and A. J. G. Hey, Phys. Lett **74B**, 77 (1978).
[5] J. S. Bell, A. C. Davis, and J. Rafelski, Phys. Lett. **78B**, 67 (1978).
[6] L. S. Celenza and C. M. Shakin, Phys. Rev. C **27**, 1561 (1983); **39**, 2477(E) (1989).

[7] C. J. Benesh and G. A. Miller, Phys. Rev. D **36**, 1344 (1987).
[8] C. J. Benesh and G. A. Miller, Phys. Lett. B **215**, 381 (1988).
[9] C. J. Benesh and G. A. Miller, Phys. Rev. D **38**, 48 (1988).
[10] C. J. Benesh and G. A. Miller, Phys. Lett. B **222**, 476 (1989).
[11] A. I. Signal and A. W. Thomas, Prog. Nucl. Part. Phys. **20**, 283 (1988).
[12] A. I. Signal and A. W. Thomas, Phys. Lett. B **211**, 481 (1988).
[13] A. I. Signal and A. W. Thomas, Phys. Rev. D **40**, 2832 (1989).
[14] F. E. Close and A. W. Thomas, Phys. Lett. B **212**, 227 (1988).
[15] A. W. Schreiber, A. W. Thomas, and J. T. Londergan, Phys. Rev. D **42**, 2226 (1990).
[16] A. I. Signal, A. W. Thomas, and A. W. Schreiber, Mod. Phys. Lett. A **6**, 271 (1991).
[17] T. Muta, *Foundations of Quantum Chromodynamics* (World Scientific, Singapore, 1987).
[18] R. L. Jaffe, in *Relativistic Dynamics and Quark-Nuclear Physics,* Proceedings of the Workshop, Los Alamos, New Mexico, 1985, edited by M. B. Johnson and A. Pickleseimer (Wiley, New York, 1985).
[19] R. L. Jaffe, Nucl Phys. **B229**, 205 (1983).
[20] R. E. Peierls and J. Yoccoz, Proc. Phys. Soc. **A70**, 381 (1957).
[21] R. E. Peierls and D. J. Thouless, Nucl. Phys. **38**, 154 (1962).
[22] F. E. Close, *An Introduction to Quarks and Partons* (Academic, New York, 1979).
[23] H. Meyer and P. J. Mulders, Nucl. Phys. **A** (to be published).
[24] K. Charchula, M. Krawczyk, H. Abramowicz, and A. Levy, ZEUS Technical Report No. 89-121, 1989.
[25] E. Eichten, I. Hinchliffe, K. Lane, and C. Quigg, Rev. Mod. Phys. **56**, 579, (1986); **58**, 1065(E) (1986).
[26] A. Martin, R. G. Roberts, and W. J. Stirling, Phys. Rev. D **37**, 1161 (1988).
[27] D. W. Duke and J. T. Owens, Phys. Rev. D **30**, 49 (1984).
[28] M. Diemoz, F. Ferroni, E. Longo, and G. Martinelli, Z. Phys. C **39**, 21 (1988).
[29] M. Glück and E. Reya, Nucl. Phys. **B130**, 76 (1977).
[30] A. I. Signal and A. W. Thomas, Phys. Lett. B **191**, 205 (1987).
[31] EMC, J. Ashman *et al.*, Phys. Lett. B **206**, 364 (1988).
[32] EMC, J. Ashman *et al.*, Nucl. Phys. **B328**, 1 (1989).
[33] A. V. Efremov and O. V. Terjaev, Dubna Report No. E2-88-287, 1988.
[34] G. Altarelli and G. G. Ross, Phys. Lett. B **212**, 391 (1988).
[35] G. Altarelli and W. J. Stirling, Particle World **1**, 40 (1989).
[36] R. D. Carlitz, J. C. Collins, and A. H. Mueller, Phys. Lett. B **214**, 229 (1989).
[37] S. L. Adler, Phys. Rev. **177**, 2426 (1969).
[38] J. S. Bell and R. Jackiw, Il Nuovo Cimento A **60**, 47 (1969).
[39] M. Glück and E. Reya, Z. Phys. C **43**, 679 (1989).
[40] M. Glück, E. Reya, and W. Vogelsang, Nucl. Phys. **B329**, 347 (1990).
[41] R. L. Jaffe and A. V. Manohar, Nucl Phys. **B337**, 509 (1990).
[42] A. V. Manohar, Phys. Rev. Lett. **66**, 289 (1991).
[43] S. D. Bass, B. L. Ioffe, N. N. Nikolaev, and A. W. Thomas, J. Moscow Phys. Soc. (to be published).
[44] A. W. Schreiber, A. W. Thomas, and J. T. Londergan, Phys. Lett. B **237**, 120 (1990).